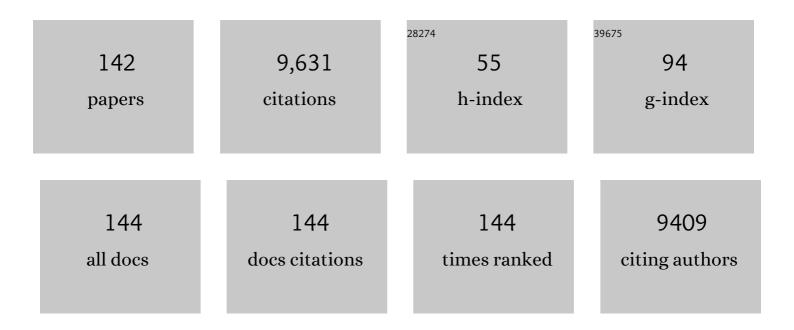
## Changha Lee

List of Publications by Year in descending order

Source: https://exaly.com/author-pdf/2588453/publications.pdf Version: 2024-02-01



#	Article	IF	CITATIONS
1	Visible-light photocatalysis over MIL-53(Fe) for VOC removal and viral inactivation in air. Environmental Engineering Research, 2022, 27, 210209-0.	2.5	5
2	Practical scale evaluation of a photocatalytic air purifier equipped with a Titania-zeolite composite bead filter for VOC removal and viral inactivation. Environmental Research, 2022, 204, 112036.	7.5	14
3	Bicarbonate-enhanced generation of hydroxyl radical by visible light-induced photocatalysis of H2O2 over WO3: Alteration of electron transfer mechanism. Chemical Engineering Journal, 2022, 432, 134401.	12.7	14
4	Efficient bicarbonate removal and recovery of ammonium bicarbonate as CO2 utilization using flow-electrode capacitive deionization. Chemical Engineering Journal, 2022, 431, 134233.	12.7	16
5	Fabrication of Ag-doped ZnO/PAN composite nanofibers by electrospinning: Photocatalytic and antiviral activities. Korean Journal of Chemical Engineering, 2022, 39, 1632-1640.	2.7	11
6	Catalytic persulfate activation for oxidation of organic pollutants: A critical review on mechanisms and controversies. Journal of Environmental Chemical Engineering, 2022, 10, 107654.	6.7	32
7	Improvement in the desalination performance of membrane capacitive deionization with a bipolar electrode via an energy recovery process. Chemical Engineering Journal, 2022, 439, 135603.	12.7	9
8	Yolk–shell-type gold nanosphere-encapsulated mesoporous silica for catalytic oxidation of organic pollutants in the presence of persulfate. Environmental Science: Nano, 2022, 9, 2510-2520.	4.3	7
9	The Photo-Fenton System. Springer Handbooks, 2022, , 1719-1734.	0.6	1
10	Selective fluoride removal in capacitive deionization by reduced graphene oxide/hydroxyapatite composite electrode. Journal of Colloid and Interface Science, 2021, 581, 396-402.	9.4	50
11	Nafion-coated Prussian blue electrodes to enhance the stability and efficiency of battery desalination system. Desalination, 2021, 500, 114778.	8.2	18
12	Hand-ground fullerene-nanodiamond composite for photosensitized water treatment and photodynamic cancer therapy. Journal of Colloid and Interface Science, 2021, 587, 101-109.	9.4	12
13	Prediction of Oxidant Exposures and Micropollutant Abatement during Ozonation Using a Machine Learning Method. Environmental Science & Technology, 2021, 55, 709-718.	10.0	21
14	Synergistic effects between the S-TiO2 photocatalyst and the Fenton-like reagent: Enhanced contaminant oxidation under visible light illumination. Journal of Environmental Chemical Engineering, 2021, 9, 104598.	6.7	11
15	Long-term and stable antimicrobial properties of immobilized Ni/TiO2 nanocomposites against Escherichia coli, Legionella thermalis, and MS2 bacteriophage. Environmental Research, 2021, 194, 110657.	7.5	8
16	Chloride-Mediated Enhancement in Heat-Induced Activation of Peroxymonosulfate: New Reaction Pathways for Oxidizing Radical Production. Environmental Science & Technology, 2021, 55, 5382-5392.	10.0	86
17	Effects of chloride and other anions on electrochemical chlorine evolution over self-doped TiO2 nanotube array. Korean Journal of Chemical Engineering, 2021, 38, 756-762.	2.7	0
18	Persulfate enhanced photoelectrochemical oxidation of organic pollutants using self-doped TiO2nanotube arrays: Effect of operating parameters and water matrix. Water Research, 2021, 191, 116803.	11.3	34

#	Article	IF	CITATIONS
19	Effect of Fe3+ as an electron-transfer mediator on WO3-induced activation of peroxymonosulfate under visible light. Chemical Engineering Journal, 2021, 411, 128529.	12.7	19
20	Degradation of aqueous organic pollutants using an Fe2O3/WO3 composite photocatalyst as a magnetically separable peroxymonosulfate activator. Separation and Purification Technology, 2021, 267, 118610.	7.9	19
21	Occurrence of unknown reactive species in UV/H2O2 system leading to false interpretation of hydroxyl radical probe reactions. Water Research, 2021, 201, 117338.	11.3	18
22	Degradation of ranitidine and changes in N-nitrosodimethylamine formation potential by advanced oxidation processes: Role of oxidant speciation and water matrix. Water Research, 2021, 203, 117495.	11.3	13
23	Ir0.11Fe0.2500.64 as a highly efficient electrode for electrochlorination in dilute chloride solutions. Journal of Industrial and Engineering Chemistry, 2021, 102, 155-162.	5.8	9
24	Nonradical activation of peroxymonosulfate by hematite for oxidation of organic compounds: A novel mechanism involving high-valent iron species. Chemical Engineering Journal, 2021, 426, 130743.	12.7	42
25	High chlorine evolution performance of electrochemically reduced TiO <sub>2</sub> nanotube array coated with a thin RuO <sub>2</sub> layer by the self-synthetic method. RSC Advances, 2021, 11, 12107-12116.	3.6	4
26	New method for electrochemical ion separation (ElONS) for chloride/nitrate separation using Ag/AgCl electrodes with a cation exchange membrane. Journal of Environmental Chemical Engineering, 2021, 9, 106876.	6.7	6
27	Use of High-Valent Metal Species Produced by the Fenton (-like) Reactions in Water Treatment. Advances in Science, Technology and Innovation, 2020, , 89-89.	0.4	0
28	Inactivation of bacterial planktonic cells and biofilms by Cu(II)-activated peroxymonosulfate in the presence of chloride ion. Chemical Engineering Journal, 2020, 380, 122468.	12.7	28
29	Novel activation of peroxymonosulfate by biochar derived from rice husk toward oxidation of organic contaminants in wastewater. Journal of Water Process Engineering, 2020, 33, 101037.	5.6	64
30	Modeling of ozone decomposition, oxidant exposures, and the abatement of micropollutants during ozonation processes. Water Research, 2020, 169, 115230.	11.3	31
31	Reduction of chlorendic acid by zero-valent iron: Kinetics, products, and pathways. Journal of Hazardous Materials, 2020, 384, 121269.	12.4	6
32	Selective phosphate removal using layered double hydroxide/reduced graphene oxide (LDH/rGO) composite electrode in capacitive deionization. Journal of Colloid and Interface Science, 2020, 564, 1-7.	9.4	68
33	Comment on "Visible-light-driven, hierarchically heterostructured, and flexible silver/bismuth oxyiodide/titania nanofibrous membranes for highly efficient water disinfection―by Song et al Journal of Colloid and Interface Science, 2020, 566, 513-514.	9.4	1
34	Nickel–Nickel oxide nanocomposite as a magnetically separable persulfate activator for the nonradical oxidation of organic contaminants. Journal of Hazardous Materials, 2020, 388, 121767.	12.4	29
35	Activation of Hydrogen Peroxide by a Titanium Oxide-Supported Iron Catalyst: Evidence for Surface Fe(IV) and Its Selectivity. Environmental Science & Technology, 2020, 54, 15424-15432.	10.0	44
36	Cupric ion in combination with hydrogen peroxide and hydroxylamine applied to inactivation of different microorganisms. Journal of Hazardous Materials, 2020, 400, 123305.	12.4	10

#	Article	IF	CITATIONS
37	Versatile Yolk–Shell Encapsulation: Catalytic, Photothermal, and Sensing Demonstration. Small, 2020, 16, e2002311.	10.0	19
38	Accelerated oxidation of microcystin-LR by Fe(II)-tetrapolyphosphate/oxygen in the presence of magnesium and calcium ions. Water Research, 2020, 184, 116172.	11.3	2
39	Freezing-enhanced non-radical oxidation of organic pollutants by peroxymonosulfate. Chemical Engineering Journal, 2020, 388, 124226.	12.7	17
40	Performance analysis of the multi-channel membrane capacitive deionization with porous carbon electrode stacks. Desalination, 2020, 479, 114315.	8.2	29
41	Visible light-induced activation of peroxymonosulfate in the presence of ferric ions for the degradation of organic pollutants. Separation and Purification Technology, 2020, 240, 116620.	7.9	27
42	Short Review of Multichannel Membrane Capacitive Deionization: Principle, Current Status, and Future Prospect. Applied Sciences (Switzerland), 2020, 10, 683.	2.5	33
43	Inactivation of Escherichia coli and MS2 coliphage via singlet oxygen generated by homogeneous photosensitization. Korean Journal of Chemical Engineering, 2019, 36, 1785-1790.	2.7	3
44	Novel Reuse Strategy in Flow-Electrode Capacitive Deionization with Switch Cycle Operation To Enhance Desalination Performance. Environmental Science and Technology Letters, 2019, 6, 739-744.	8.7	15
45	Enhancement in Desalination Performance of Battery Electrodes via Improved Mass Transport Using a Multichannel Flow System. ACS Applied Materials & Interfaces, 2019, 11, 36580-36588.	8.0	30
46	Ag-doped graphitic carbon nitride photocatalyst with remarkably enhanced photocatalytic activity towards antibiotic in hospital wastewater under solar light. Journal of Industrial and Engineering Chemistry, 2019, 80, 597-605.	5.8	46
47	Differential Microbicidal Effects of Bimetallic Iron–Copper Nanoparticles on <i>Escherichia coli</i> and MS2 Coliphage. Environmental Science & Technology, 2019, 53, 2679-2687.	10.0	31
48	Ozonation of Microcystins: Kinetics and Toxicity Decrease. Environmental Science & Technology, 2019, 53, 6427-6435.	10.0	17
49	Electrochemical oxidation of organics in sulfate solutions on boron-doped diamond electrode: Multiple pathways for sulfate radical generation. Applied Catalysis B: Environmental, 2019, 254, 156-165.	20.2	91
50	Spontaneous Generation of H <sub>2</sub> O <sub>2</sub> and Hydroxyl Radical through O <sub>2</sub> Reduction on Copper Phosphide under Ambient Aqueous Condition. Environmental Science & Technology, 2019, 53, 2918-2925.	10.0	88
51	Effect of Hydrophilicity of Activated Carbon Electrodes on Desalination Performance in Membrane Capacitive Deionization. Applied Sciences (Switzerland), 2019, 9, 5055.	2.5	18
52	La-modified ZSM-5 zeolite beads for enhancement in removal and recovery of phosphate. Microporous and Mesoporous Materials, 2019, 279, 37-44.	4.4	64
53	Activation of Periodate by Freezing for the Degradation of Aqueous Organic Pollutants. Environmental Science & Technology, 2018, 52, 5378-5385.	10.0	101
54	Oxidation of organic pollutants by peroxymonosulfate activated with low-temperature-modified nanodiamonds: Understanding the reaction kinetics and mechanism. Applied Catalysis B: Environmental, 2018, 237, 432-441.	20.2	161

#	Article	IF	CITATIONS
55	Nitrite ion mitigates the formation of N-nitrosodimethylamine (NDMA) during chloramination of ranitidine. Science of the Total Environment, 2018, 633, 352-359.	8.0	19
56	Comment on "Investigation of the Iron–Peroxo Complex in the Fenton Reaction: Kinetic Indication, Decay Kinetics, and Hydroxyl Radical Yields― Environmental Science & Technology, 2018, 52, 4481-4482.	10.0	1
5 <b>7</b>	Synchronized methylene blue removal using Fenton-like reaction induced by phosphorous oxoanion and submerged plasma irradiation process. Journal of Environmental Management, 2018, 206, 77-84.	7.8	14
58	Chloride-enhanced oxidation of organic contaminants by Cu(II)-catalyzed Fenton-like reaction at neutral pH. Journal of Hazardous Materials, 2018, 344, 1174-1180.	12.4	81
59	Visible light-photosensitized oxidation of organic pollutants using amorphous peroxo-titania. Applied Catalysis B: Environmental, 2018, 225, 487-495.	20.2	27
60	Oxidation of Microcystins by Permanganate: pH and Temperature-Dependent Kinetics, Effect of DOM Characteristics, and Oxidation Mechanism Revisited. Environmental Science & Technology, 2018, 52, 7054-7063.	10.0	39
61	Electrochemical Peroxodisulfate (PDS) Generation on a Self-Doped TiO <sub>2</sub> Nanotube Array Electrode. Industrial & Engineering Chemistry Research, 2018, 57, 11465-11471.	3.7	23
62	Binder-free immobilization of TiO2 photocatalyst on steel mesh via electrospraying and hot-pressing and its application for organic micropollutant removal and disinfection. Journal of Hazardous Materials, 2018, 360, 62-70.	12.4	16
63	Enhanced Oxidation of Phenol by Copper-catalyzed Fenton-like Reaction in the Presence of Bicarbonate. Journal of Advanced Oxidation Technologies, 2018, 21, 54-66.	0.5	5
64	Accelerated redox reaction between chromate and phenolic pollutants during freezing. Journal of Hazardous Materials, 2017, 329, 330-338.	12.4	41
65	Oxidation of microcystin-LR by ferrous-tetrapolyphosphate in the presence of oxygen and hydrogen peroxide. Water Research, 2017, 114, 277-285.	11.3	34
66	Reply to comment on "Combination of cupric ion with hydroxylamine and hydrogen peroxide for the control of bacterial biofilms on RO membranes by Hye-Jin Lee, Hyung-Eun Kim, Changha Lee [Water Research 110, 2017, 83–90]― Water Research, 2017, 118, 291-292.	11.3	0
67	Response to Comment on "Activation of Persulfate by Graphitized Nanodiamonds for Removal of Organic Compounds†Environmental Science & Technology, 2017, 51, 5353-5354.	10.0	18
68	Nanoparticulate zero-valent iron coupled with polyphosphate: the sequential redox treatment of organic compounds and its stability and bacterial toxicity. Environmental Science: Nano, 2017, 4, 396-405.	4.3	10
69	Combination of cupric ion with hydroxylamine and hydrogen peroxide for the control of bacterial biofilms on RO membranes. Water Research, 2017, 110, 83-90.	11.3	34
70	Inactivation of biofilms on RO membranes by copper ion in combination with norspermidine. Desalination, 2017, 424, 95-101.	8.2	10
71	Adsorption of As(V) by boehmite and alumina of different morphologies prepared under hydrothermal conditions. Chemosphere, 2017, 169, 99-106.	8.2	53
72	Visible-light-induced activation of periodate that mimics dye-sensitization of TiO2: Simultaneous decolorization of dyes and production of oxidizing radicals. Applied Catalysis B: Environmental, 2017, 203, 475-484.	20.2	97

#	Article	IF	CITATIONS
73	Control of the red tide dinoflagellate Cochlodinium polykrikoides by ozone in seawater. Water Research, 2017, 109, 237-244.	11.3	15
74	Science Walden: Exploring the Convergence of Environmental Technologies with Design and Art. Sustainability, 2017, 9, 35.	3.2	1
75	Activation of Oxygen and Hydrogen Peroxide by Copper(II) Coupled with Hydroxylamine for Oxidation of Organic Contaminants. Environmental Science & amp; Technology, 2016, 50, 8231-8238.	10.0	166
76	Activation of Persulfates by Graphitized Nanodiamonds for Removal of Organic Compounds. Environmental Science & Technology, 2016, 50, 10134-10142.	10.0	546
77	Highly reusable TiO 2 nanoparticle photocatalyst by direct immobilization on steel mesh via PVDF coating, electrospraying, and thermal fixation. Chemical Engineering Journal, 2016, 306, 344-351.	12.7	57
78	Activation of Peroxymonosulfate by Surface-Loaded Noble Metal Nanoparticles for Oxidative Degradation of Organic Compounds. Environmental Science & Technology, 2016, 50, 10187-10197.	10.0	262
79	Disintegration of Waste Activated Sludge by Thermally-Activated Persulfates for Enhanced Dewaterability. Environmental Science & Technology, 2016, 50, 7106-7115.	10.0	223
80	Oxidative treatment of waste activated sludge by different activated persulfate systems for enhancing sludge dewaterability. Sustainable Environment Research, 2016, 26, 177-183.	4.2	41
81	Electrochemical ozone production in inert supporting electrolytes on a boron-doped diamond electrode with a solid polymer electrolyte electrolyzer. Desalination and Water Treatment, 2016, 57, 10152-10158.	1.0	15
82	Enhanced Inactivation of <i>Escherichia coli</i> and MS2 Coliphage by Cupric Ion in the Presence of Hydroxylamine: Dual Microbicidal Effects. Environmental Science & Technology, 2015, 49, 14416-14423.	10.0	57
83	Reaction of aqueous iodide at high concentration with O3 and O3/H2O2 in the presence of natural organic matter: implications for drinking water treatment. Environmental Chemistry Letters, 2015, 13, 453-458.	16.2	15
84	Activation of persulfates by carbon nanotubes: Oxidation of organic compounds by nonradical mechanism. Chemical Engineering Journal, 2015, 266, 28-33.	12.7	556
85	Fate of engineered nanoparticles: Implications in the environment. Coordination Chemistry Reviews, 2015, 287, 64-78.	18.8	171
86	Distinctive green recovery of silver species from modified cellulose: Mechanism and spectroscopic studies. International Journal of Biological Macromolecules, 2015, 76, 109-118.	7.5	10
87	Polyphosphate-enhanced production of reactive oxidants by nanoparticulate zero-valent iron and ferrous ion in the presence of oxygen: Yield and nature of oxidants. Water Research, 2015, 86, 66-73.	11.3	56
88	Distinct adsorption enhancement of bi-component metals (cobalt and nickel) by Fireweed-derived carbon compared to activated carbon: Incorporation of surface group distributions for increased efficiency. Chemical Engineering Journal, 2015, 281, 713-723.	12.7	29
89	Substrate-immobilized electrospun TiO2 nanofibers for photocatalytic degradation of pharmaceuticals: The effects of pH and dissolved organic matter characteristics. Water Research, 2015, 86, 25-34.	11.3	66
90	Synthesis and characterization of metal-doped reduced graphene oxide composites, and their application in removal of Escherichia coli, arsenic and 4-nitrophenol. Journal of Industrial and Engineering Chemistry, 2015, 29, 282-288.	5.8	57

#	Article	IF	CITATIONS
91	Enhanced production of reactive oxidants by Fenton-like reactions in the presence of carbon materials. Chemical Engineering Journal, 2015, 273, 502-508.	12.7	77
92	Photocatalytic applications of paper-like poly(vinylidene fluoride)–titanium dioxide hybrids fabricated using a combination of electrospinning and electrospraying. Journal of Hazardous Materials, 2015, 285, 267-276.	12.4	59
93	Effects of inorganic oxidants on kinetics and mechanisms of WO 3 -mediated photocatalytic degradation. Applied Catalysis B: Environmental, 2015, 162, 515-523.	20.2	79
94	Oxidation of organic contaminants in water by iron-induced oxygen activation: A short review. Environmental Engineering Research, 2015, 20, 205-211.	2.5	31
95	Effects of advanced treatments using granular activated carbon adsorption with ozonation and ultrafiltration on chlorine decay. Desalination and Water Treatment, 2014, 52, 976-984.	1.0	2
96	Raspberry derived mesoporous carbon-tubules and fixed-bed adsorption of pharmaceutical drugs. Journal of Industrial and Engineering Chemistry, 2014, 20, 1126-1132.	5.8	56
97	Oxidant production from corrosion of nano- and microparticulate zero-valent iron in the presence of oxygen: A comparative study. Journal of Hazardous Materials, 2014, 265, 201-207.	12.4	57
98	Degradation of diclofenac and carbamazepine by the copper(II)-catalyzed dark and photo-assisted Fenton-like systems. Chemical Engineering Journal, 2014, 245, 258-264.	12.7	118
99	Synthesis of graphene–carbon sphere hybrid aerogel with silver nanoparticles and its catalytic and adsorption applications. Chemical Engineering Journal, 2014, 244, 160-167.	12.7	100
100	Electrochromic titania nanotube arrays for the enhanced photocatalytic degradation of phenol and pharmaceutical compounds. Chemical Engineering Journal, 2014, 249, 285-292.	12.7	57
101	Single-step green synthesis of imine-functionalized carbon spheres and their application in uranium removal from aqueous solution. RSC Advances, 2014, 4, 46114-46121.	3.6	20
102	Oxidizing Capacity of Periodate Activated with Iron-Based Bimetallic Nanoparticles. Environmental Science & Technology, 2014, 48, 8086-8093.	10.0	133
103	Visible light photoelectrocatalytic degradation of methyl orange using anodized nanoporous WO3. Electrochimica Acta, 2014, 115, 140-145.	5.2	40
104	Kinetic enhancement in photocatalytic oxidation of organic compounds by WO3 in the presence of Fenton-like reagent. Applied Catalysis B: Environmental, 2013, 138-139, 311-317.	20.2	56
105	Use of CaO as an activator for producing a price-competitive non-cement structural binder using ground granulated blast furnace slag. Cement and Concrete Research, 2013, 54, 208-214.	11.0	320
106	Protocol for development of various plants leaves extract in single-pot synthesis of metal nanoparticles. Spectrochimica Acta - Part A: Molecular and Biomolecular Spectroscopy, 2013, 103, 134-142.	3.9	37
107	pH-Dependent reactivity of oxidants formed by iron and copper-catalyzed decomposition of hydrogen peroxide. Chemosphere, 2013, 92, 652-658.	8.2	160
108	Microbial Inactivation by Cupric Ion in Combination with H <sub>2</sub> O <sub>2</sub> : Role of Reactive Oxidants. Environmental Science & Technology, 2013, 47, 13661-13667.	10.0	81

#	Article	IF	CITATIONS
109	Magnetite/mesocellular carbon foam as a magnetically recoverable fenton catalyst for removal of phenol and arsenic. Chemosphere, 2012, 89, 1230-1237.	8.2	76
110	Role of Reactive Oxygen Species in <i>Escherichia coli</i> Inactivation by Cupric Ion. Environmental Science & Technology, 2012, 46, 11299-11304.	10.0	72
111	Carbon nanotube-based membranes: Fabrication and application to desalination. Journal of Industrial and Engineering Chemistry, 2012, 18, 1551-1559.	5.8	165
112	Synergistic effects of TiO2 photocatalysis in combination with Fenton-like reactions on oxidation of organic compounds at circumneutral pH. Applied Catalysis B: Environmental, 2012, 115-116, 219-224.	20.2	78
113	Photosensitized Oxidation of Emerging Organic Pollutants by Tetrakis C <sub>60</sub> Aminofullerene-Derivatized Silica under Visible Light Irradiation. Environmental Science & Technology, 2011, 45, 10598-10604.	10.0	107
114	Inactivation of MS2 Coliphage by Ferrous Ion and Zero-Valent Iron Nanoparticles. Environmental Science & Technology, 2011, 45, 6978-6984.	10.0	114
115	Comment on "Oxidation of Sulfoxides and Arsenic(III) in Corrosion of Nanoscale Zero Valent Iron by Oxygen: Evidence against Ferryl Ions (Fe(IV)) as Active Intermediates in Fenton Reactionâ€. Environmental Science & Technology, 2011, 45, 3177-3178.	10.0	15
116	Magnetic mesoporous materials for removal of environmental wastes. Journal of Hazardous Materials, 2011, 192, 1140-1147.	12.4	78
117	Inactivation of MS2 bacteriophage by streamer corona discharge in water. Chemosphere, 2011, 82, 1135-1140.	8.2	30
118	Decolorization of reactive dye using a photo-ferrioxalate system with brick grain-supported iron oxide. Journal of Hazardous Materials, 2011, 188, 357-362.	12.4	20
119	Inactivation of <i>Escherichia coli</i> by Nanoparticulate Zerovalent Iron and Ferrous Ion. Applied and Environmental Microbiology, 2010, 76, 7668-7670.	3.1	125
120	Inactivation of MS2 coliphage by Fenton's reagent. Water Research, 2010, 44, 2647-2653.	11.3	65
121	A novel homogeneous Fenton-like system with Fe(III)–phosphotungstate for oxidation of organic compounds at neutral pH values. Journal of Molecular Catalysis A, 2009, 311, 1-6.	4.8	98
122	A Silica-Supported Iron Oxide Catalyst Capable of Activating Hydrogen Peroxide at Neutral pH Values. Environmental Science & Technology, 2009, 43, 8930-8935.	10.0	317
123	UV direct photolysis of 2,2′-azino-bis(3-ethylbenzothiazoline-6-sulfonate) (ABTS) in aqueous solution: Kinetics and mechanism. Journal of Photochemistry and Photobiology A: Chemistry, 2008, 197, 232-238.	3.9	33
124	Enhanced Formation of Oxidants from Bimetallic Nickelâ^'Iron Nanoparticles in the Presence of Oxygen. Environmental Science & Technology, 2008, 42, 8528-8533.	10.0	118
125	Polyoxometalate-Enhanced Oxidation of Organic Compounds by Nanoparticulate Zero-Valent Iron and Ferrous Ion in the Presence of Oxygen. Environmental Science & Technology, 2008, 42, 4921-4926.	10.0	168
126	Enhanced inactivation of E. coli and MS-2 phage by silver ions combined with UV-A and visible light irradiation. Water Research, 2008, 42, 356-362.	11.3	155

#	Article	IF	CITATIONS
127	Oxidation of suspected N-nitrosodimethylamine (NDMA) precursors by ferrate (VI): Kinetics and effect on the NDMA formation potential of natural waters. Water Research, 2008, 42, 433-441.	11.3	98
128	Bactericidal Effect of Zero-Valent Iron Nanoparticles on Escherichia coli. Environmental Science & Technology, 2008, 42, 4927-4933.	10.0	667
129	Response to Comment on "Polyoxometalate-Enhanced Oxidation of Organic Compounds by Nanoparticulate Zero-Valent Iron and Ferrous Ion in the Presence of Oxygen― Environmental Science & Technology, 2008, 42, 8169-8169.	10.0	2
130	Oxidative degradation of N-nitrosodimethylamine by conventional ozonation and the advanced oxidation process ozone/hydrogen peroxide. Water Research, 2007, 41, 581-590.	11.3	216
131	Oxidation ofN-Nitrosodimethylamine (NDMA) Precursors with Ozone and Chlorine Dioxide:Â Kinetics and Effect on NDMA Formation Potential. Environmental Science & Technology, 2007, 41, 2056-2063.	10.0	223
132	UV-A induced photochemical formation of N-nitrosodimethylamine (NDMA) in the presence of nitrite and dimethylamine. Journal of Photochemistry and Photobiology A: Chemistry, 2007, 189, 128-134.	3.9	35
133	Oxidative degradation of dimethylsulfoxide by locally concentrated hydroxyl radicals in streamer corona discharge process. Chemosphere, 2006, 65, 1163-1170.	8.2	33
134	UV Photolytic Mechanism ofN-Nitrosodimethylamine in Water:Â Dual Pathways to Methylamine versus Dimethylamine. Environmental Science & Technology, 2005, 39, 2101-2106.	10.0	110
135	UV Photolytic Mechanism ofN-Nitrosodimethylamine in Water:Â Roles of Dissolved Oxygen and Solution pH. Environmental Science & Technology, 2005, 39, 9702-9709.	10.0	86
136	Application of photoactivated periodate to the decolorization of reactive dye: reaction parameters and mechanism. Journal of Photochemistry and Photobiology A: Chemistry, 2004, 165, 35-41.	3.9	89
137	Temperature dependence of hydroxyl radical formation in the hv/Fe3+/H2O2 and Fe3+/H2O2 systems. Chemosphere, 2004, 56, 923-934.	8.2	84
138	Determination of quantum yields for the photolysis of Fe(III)-hydroxo complexes in aqueous solution using a novel kinetic method. Chemosphere, 2004, 57, 1449-1458.	8.2	34
139	Kinetics and mechanisms of DMSO (dimethylsulfoxide) degradation by UV/H2O2 process. Water Research, 2004, 38, 2579-2588.	11.3	90
140	High temperature dependence of 2,4-dichlorophenoxyacetic acid degradation by Fe 3+ /H 2 O 2 system. Chemosphere, 2003, 51, 963-971.	8.2	63
141	Influence of various reaction parameters on 2,4-D removal in photo/ferrioxalate/H 2 O 2 process. Chemosphere, 2003, 51, 901-912.	8.2	57
142	Practical selection of microorganisms indicating the stability of pathogenic removal in water treatment plants. Water Science and Technology: Water Supply, 2002, 2, 373-380.	2.1	0